Research in Astron. Astrophys. **2009** Vol. **9** No. **10**, 1155–1164
http://www.raa-journal.org *http://www.iop.org/journals/raa*

Research in Astronomy and Astrophysics

Double hard X-ray peaks in *RHESSI* flares as evidence of chromospheric evaporation and implications for modifying the Neupert effect *

You-Ping Li, Wei-Qun Gan and Yang Su

Purple Mountain Observatory, Chinese Academy of Sciences, Nanjing 210008, China;
wqgan@pmo.ac.cn

Received 2009 April 15; accepted 2009 May 15

Abstract Among the *RHESSI* flare samples, we concentrated on a kind of flare that presents two successive peaks (that is, it presents both an impulsive phase and a gradual phase) in 12 – 25 keV light curves. Taking the C1.4 flare on 2002 August 12 as an example, we studied the light curves, spectra, and images in detail. Making full use of the capabilities of *RHESSI*, we showed some evidence to support the expected causal relationship between these two peaks: the first peak is mainly nonthermal, while the second peak is mainly thermal; the energy carried by nonthermal electrons during the first peak seems to be comparable to the thermal energy of the second peak. The morphologies of X-ray images and their evolutions provide additional evidence for this causality. We conclude that two such peaks in the 12 – 25 keV light curve are good evidence for the chromospheric evaporation. However, the maximum time of the second peak is later than the end time of the first peak, suggesting that for some events, a modification of the traditional Neupert effect could be necessary by inclusion of a time delay, which might be partly related to the filling of the loop by evaporated material.

Key words: Sun: flares — Sun: X-rays, gamma-rays

1 INTRODUCTION

It is now widely accepted that a solar flare results from some kind of plasma instability in the corona, which first accelerates the electrons and ions. These energetic particles are then transported downwards along the magnetic lines and interact with ambient solar materials, emitting non-thermal radiation, like hard X-rays (HXRs) and gamma-rays (e.g., Brown 1971). Meanwhile, through Coulomb collisions, energy deposition in the solar atmosphere is transformed into thermal emission, like soft X-rays (SXRs). The so-called chromospheric evaporation (e.g., Antonucci et al. 1984; Fisher et al. 1985; Gan et al. 1991) plays a key role in transforming non-thermal input energy into thermal emissions. This traditional scenario for solar flares has found more and more observational support (e.g., Gan & Li 2002; Teriaca et al. 2003; Aschwanden 2004 and references within; Veronig et al. 2005; Liu et al. 2006; Milligan et al. 2006; Brosius & Holman 2007).

Li & Gan (2006), using the BATSE and *GOES* observations, statistically studied the peak time differences between the SXRs and HXRs. They found that the flaring loop size is the reason for the peak time difference between the SXR and HXR emissions. The longer the flaring loop is, the longer

* Supported by the National Natural Science Foundation of China.

the time for chromospheric evaporation reaching the loop top is, i.e., the later the SXR peaks appear. The traditional model of chromospheric evaporation received great support there.

In comparison with BATSE, the Reuven Ramaty High-Energy Solar Spectroscopic Imager (*RHESSI*) (Lin et al. 2002) has a higher energy resolution, a wider energy coverage down to 3 keV, and imaging ability. In flares, there are generally two X-ray increases. One, dominating hard X-rays, has a short duration and a hard spectrum (the impulsive phase) while the other, dominating soft X-rays, has a longer duration and a soft spectrum (the gradual phase). Usually, these two increases for one flare are observed at two separate energy channels by two different instruments, like HXRBS and *GOES* (e.g., Dennis & Zarro 1993) or BATSE and *GOES* (e.g., Veronig et al. 2002b; Li & Gan 2006). We may expect that for some cases, there is an intermediate photon energy range, in which both increases (impulsive phase and gradual phase) could be well observed, that is, two successive peaks could be seen, although such kind of flares might show no physical difference from the other flares which show two peaks at two separate energy channels. We checked the events observed with *RHESSI* and found that for some events, 12 – 25 keV is the intermediate photon energy range. In fact, such kind of flares had been shown and studied by Kane & Anderson (1970). Lin & Hudson (1976) explained these two peaks, which actually constitute a basic ingredient of the modern standard scenario for solar flares. However, at that time, both poor energy resolution and non-imaging capability in observations prevented them from doing further detailed studies.

In this paper, after presenting some *RHESSI* examples which show two successive peaks in the 12 – 25 keV light curves, we focus on a C1.4 flare on 2002 August 12 and make a detailed study with the full capability of *RHESSI*. The expected causal relationship between the two successive peaks in the 12 – 25 keV light curve have been checked. The standard scenario of solar flares is therefore well presented in this small flare. As last, we discuss the limitation of the traditional Neupert effect and propose that the traditional Neupert effect should be modified by including a time delay.

2 SOME EXAMPLES OF TWO PEAKS IN 12 – 25 keV LIGHT CURVES

Figure 1 shows the light curves of 6 – 12, 12 – 25 and 25 – 50 keV for the six example flares observed with *RHESSI*, together with the *GOES* light curves at 0.5 – 4 Å (thick dotted line, background-subtracted) and 1 – 8 Å (thin dotted line, background-subtracted). The common features of these flares, that is, the criteria for selecting these samples, are that both the impulsive phase and gradual phase can be seen in the 12 – 25 keV light curves. The time difference between the two peaks is in tens of seconds. For the energy channel higher than 25 keV, however, we can distinguish only the first peak. On the other hand, the first peak cannot be distinguished in the *GOES* 1 – 8 Å light curves. Presumably, they are all examples of "early impulsive flares" as defined by Sui et al. (2006). The *RHESSI* examples presented in the figure are similar to early observations by Kane & Anderson (1970).

It is generally thought that emission above 25 keV comes mostly from non-thermal bremsstrahlung, and that below 10 keV mostly from thermal bremsstrahlung. Between 10 keV and 25 keV, it should, in principle, include both thermal and non-thermal contributions (e.g., Aschwanden 2007). If the standard model of solar flares plays a role, there should be some connection between these two peaks. In the following sections, we will study a small flare in Figure 1 in detail. This small sample event allows us to go further and test details of chromospheric evaporation in a novel way not possible for larger and more complex events.

3 THE C1.4 FLARE ON 2002 AUGUST 12

According to *GOES*, the C1.4 flare on 2002 August 12 began at 02:16 UT and peaked at 02:19 UT. Since no attenuators (Smith et al. 2002) were set in front of the detectors during the flare, emissions as low as 3 keV were well observed by *RHESSI*. In order to obtain a high temporal resolution light curve, we demodulated the time profiles (by using the command hsi_demodulator in the *RHESSI* software) with a time resolution of 0.1 s for summing the front detectors of 1F, 3F-6F, 8F, and 9F. Within 3 to 27 keV, 12 channels were binned with 2 keV for each step. The smoothed light curves, after filtering out the high

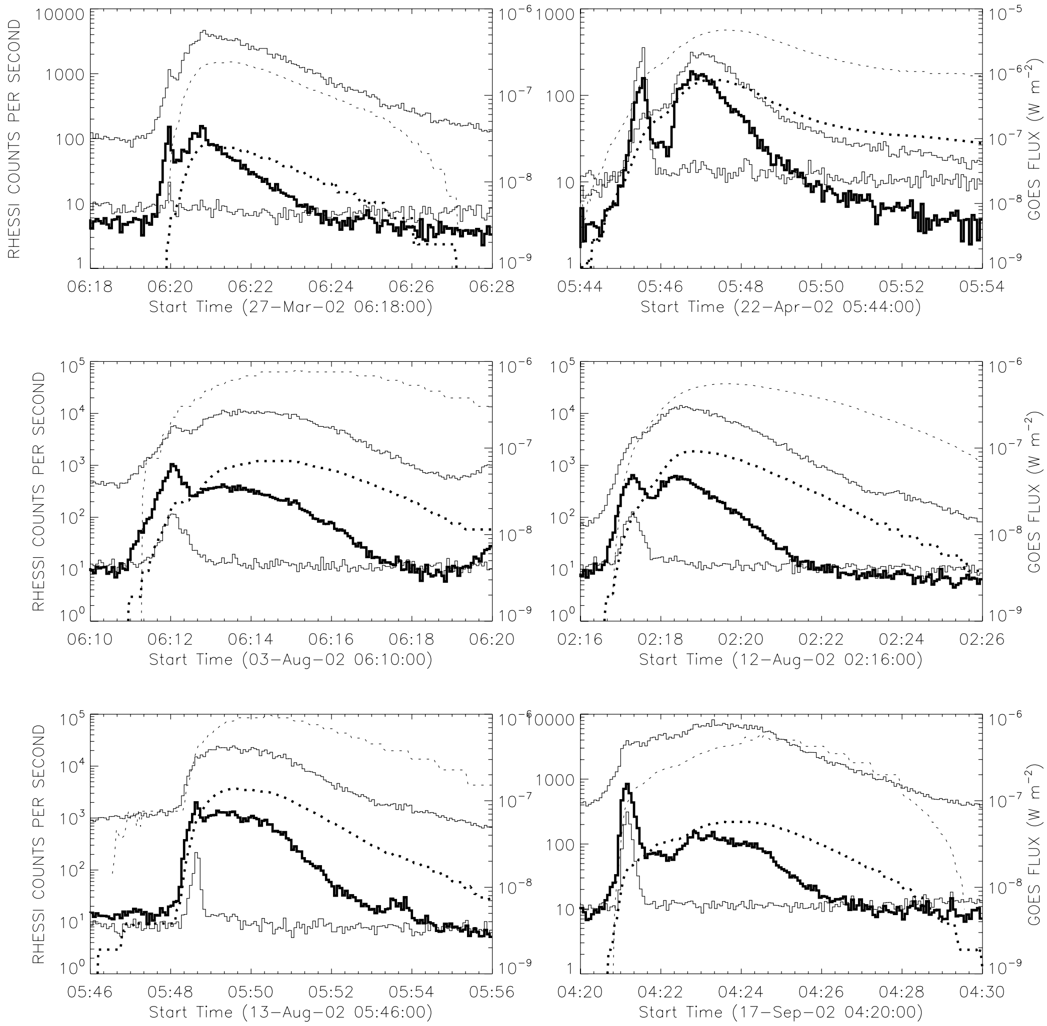

Fig. 1 *RHESSI* (thin solid lines for 6 – 12 and 25 – 50 keV; thick ones for 12 – 25 keV) and *GOES* (background-subtracted, thin dotted lines for 1 – 8 Å and thick ones for 0.5 – 4 Å) light curves of the six example events.

frequency components (by Fourier transform filtering with the IDL BUTTERWORTH lowpass filter, choosing the parameters cutoff as 5 and order as 2), as shown in Figure 2. Two peaks, with a time difference varying with the energy, are very obvious in the channel between 11 keV and 19 keV. For the first peak, the peak time in different energy channels is nearly the same, but below 11 keV the peak cannot be distinguished. For the second peak, it can only be distinguished below 19 keV. The peak time delay with decreasing energies is very obvious for the second peak. This energy-dependent time delay indicates a multi-temperature plasma with cooling dominated by thermal conduction (Aschwanden 2007).

The *RHESSI* spatially integrated spectra at two peak time intervals are shown in the bottom of Figure 2, where all the front detectors except 2F and 7F were summed. As expected, we see from the figure that the non-thermal component is dominant at the first peak, while the thermal (multi-thermal) component is dominant at the second peak. It is also noted that the fitting with a multi-thermal model is

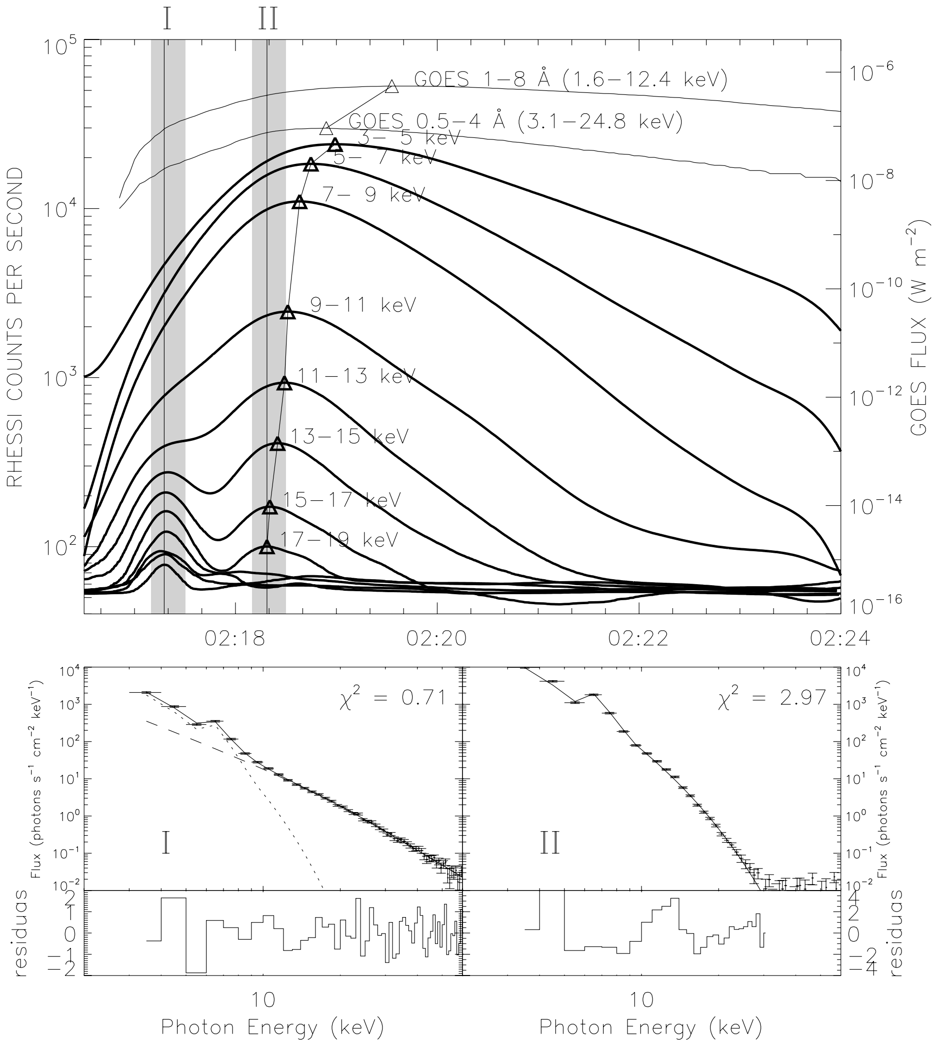

Fig. 2 *Top*: *RHESSI* (*thick lines*) and *GOES* (*thin lines*) light curves for the C1.4 flare on 2002 August 12. The vertical lines indicate the times when the 17 – 19 keV flux peaks happened. The triangular symbols mark the peak times for different energy bands at the second peak. The shadows designated by 'I' and 'II' indicate the 20 s time intervals for each peak. *Bottom*: *RHESSI* spatially integrated spectra in two time intervals and their fitting results. The fitting model for peak 'I' is an isothermal component plus a power-law nonthermal component, while for peak 'II' a multi-power-law thermal model is used.

better than that with a single-thermal model for the second peak. This fact supports the explanation of Aschwanden (2007) who argued that the peak time delay comes from the multi-thermal cooling.

Morphologically, Figure 3 shows the images at 3 – 6 keV, 6 – 12 keV, and 12 – 25 keV for the two peaks. The CLEAN algorithm (Hurford et al. 2002) was used in the reconstruction of these images for grids 3F–8F except 7F. The white/black contours in the figure are the images of 25 – 50 keV for the first peak, which presents an intensity asymmetry of the two footpoints (Jin & Ding 2007). For the first peak, we seem to see the whole loop, but the lower energy X-ray footpoint source (6 – 12 keV) is higher in altitude than the higher energy footpoint source (12 – 25 keV) by about 1500 km. This reflects the

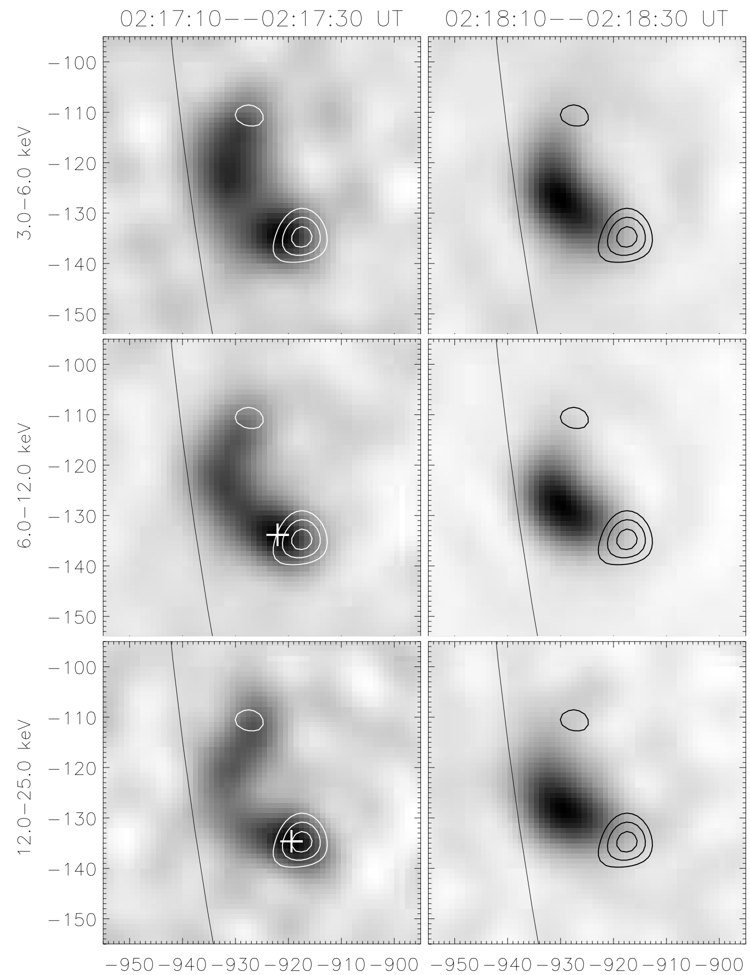

Fig. 3 *RHESSI* images (inverse color) for three energy bands overlayed on the white/black contours (25 – 50 keV at 02:17:10 – 02:17:30 UT for 50%, 70% and 90% of the peak flux) for two peak time intervals 'I' and 'II.' The two plus symbols indicate the centroid of 90% contours at 6 – 12 keV and 12 – 25 keV.

nonthermal property (Aschwanden et al. 2002) and is qualitatively consistent with the so-called "early impulsive flare" discovered by Sui et al. (2006, 2007). For the second peak, we only see the looptop source rather than the footpoint source. In addition, the looptop source cannot be seen above 25 keV. This scenario suggests that the second peak has a thermal origin.

The temporal evolution of the source at 6 – 12 keV is shown in Figure 4. The meaning of the white contours is the same as in Figure 3, but the black line is the 50% contour of the 6 – 12 keV source. The figure presents a detailed process about how the source evolves from being loop-distributed to going to the looptop: before the first peak at 02:17:20 UT the emissions from the footpoints are dominant, although the north footpoint is relatively weaker; after the first peak time, the source moves closer to the looptop. This picture is, in principle, the same as that shown by Liu et al. (2006), where they declared that the evolution of X-ray sources is as expected for the evaporation model. However, it is easily found from Figure 4 that the loop apex is already bright at the end of the first peak, suggesting that the evaporated material has already filled the loop. Why does the thermal energy continue to increase after this time?

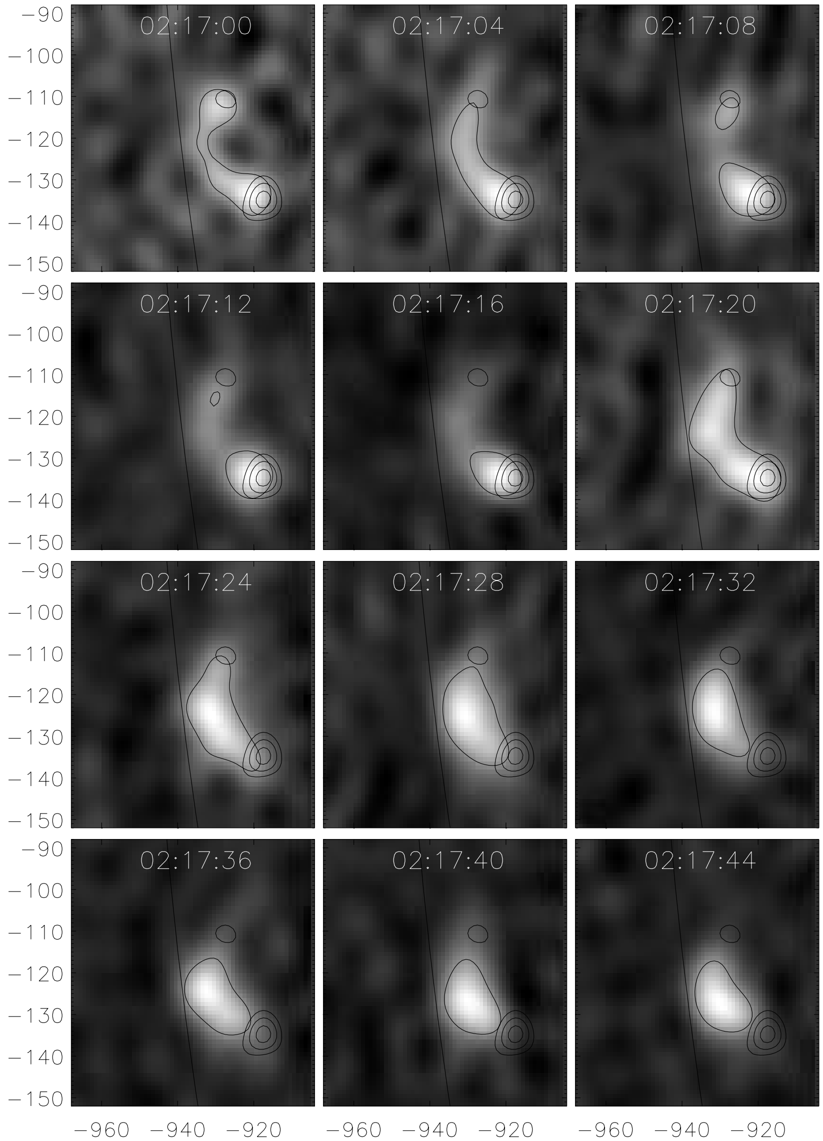

Fig. 4 *RHESSI* 6 – 12 keV images and 50% contours (*black*) at different times. The white contours (25 – 50 keV at 02:17:10 – 02:17:30 UT) show the footpoints of the loops.

One possibility is that there might be some direct heating which started before the impulsive nonthermal peak and continued on after it was over. This possibility is also suitable for explaining why the thermal X-ray flux below 10 keV starts to rise well before nonthermal emission at higher energies (see Fig. 2). Another possibility is that the first appearance of the bright loop apex corresponded to the moment when the initial evaporated material reached the looptop, and the continuous increase of the looptop brightness resulted from the later evaporated material reaching the looptop.

We then check the energetics of the impulsive and gradual phases. With the *GOES* software in SSW, the emission measure (EM) and plasma temperature (T) were derived from fitting the fluxes in two channels of *GOES*. The volume (V) was estimated from the 50% contours (e.g., Emslie et al. 2004;

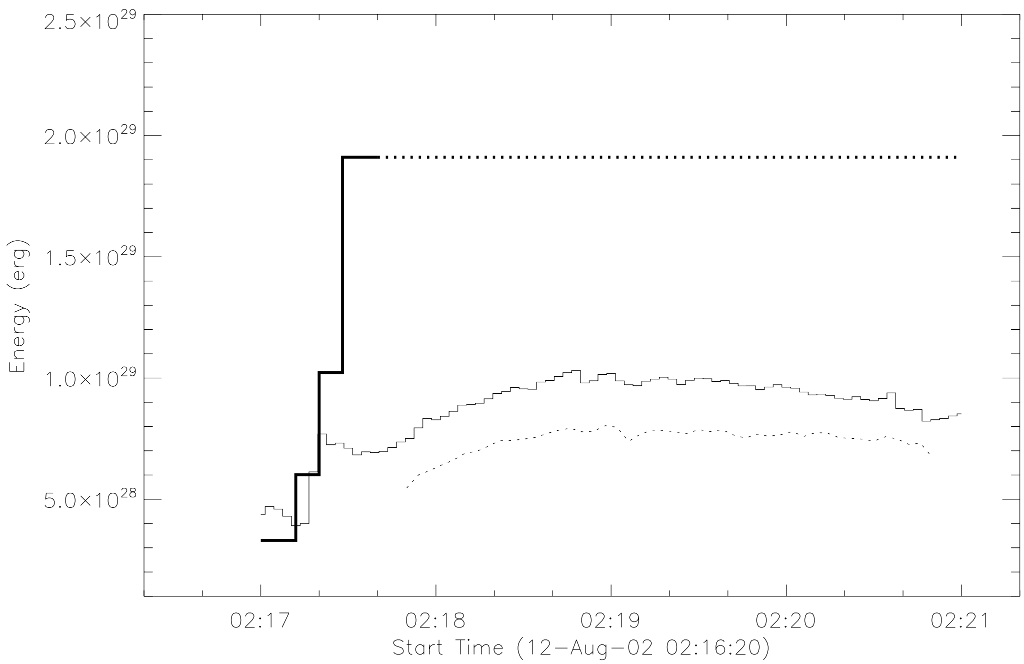

Fig. 5 Thermal plasma energy derived from *GOES* (*thin line*), the thermal plasma energy (*thin dotted line*) and the accumulated energy of nonthermal electrons (*thick line*) derived from the *RHESSI* spectral fitting. The thick dotted line is drawn for easy comparison.

Sui et al. 2005) of 6 – 12 keV images in Figure 4. Assuming a filling factor of 1, we used

$$E_{\mathrm{therm}} = 3 \times \kappa \times T \times \sqrt{\mathrm{EM} \times V}$$

to estimate the plasma thermal energy which is, in fact, an upper limit, where κ is Boltzman's constant. The result was shown in a thin histogram in Figure 5. The maximum thermal energy of about 1.0×10^{29} erg happens at 02:18:50 UT. Jiang et al. (2006) studied the cooling phase of this flare and found that the cooling time scale is about 5 minutes. Recalling the median cooling time of 6 minutes (Veronig et al. 2002a, 2002c), we neglect the energy consumption during the first 2 minutes and take this maximum energy as the total thermal energy carried by the flare.

Assuming a thermal spectrum plus a thick-target bremsstrahlung produced by power-law electrons with a sharp lower-energy cutoff (e.g., Gan et al. 2001), the 3 – 50 keV X-ray spectrum was fitted. The calculated energy (summed) carried by nonthermal electrons was shown with a thick histogram in Figure 5. The extended dotted line is drawn for a comparison without absolute meaning. The calculated total energy carried by nonthermal electrons is about 1.9×10^{29} erg, which happens mainly during the first peak. In Figure 5, the thermal energies derived from *RHESSI* after 02:17:50 UT were also shown in a thin dotted line, which seem to be comparable to those obtained from *GOES*. This confirms the work by Sui et al. (2005), who stated that the thermal energies obtained with *GOES* and *RHESSI* are almost equal to each other. The energy uncertainty of nonthermal electrons mainly depends on the uncertainty of the lower-energy cutoff. In the spectral fitting, we let the lower energy cutoff be a free parameter. However, since the nonthermal spectrum is increasingly dominated by the thermal spectrum at lower energies and the lower-energy cutoff of the electron spectrum could be significantly lower than the best fit value, as pointed out by Holman et al. (2003), the nonthermal energies derived in this way could therefore be considered as lower limits. This acquired nonthermal energy is notably comparable to 1.4×10^{29} erg obtained by Jiang et al. (2006), who studied the energy deposition only at the footpoints of the flare around the first peak time.

As is the case for many more complex flares (e.g., Dennis et al. 2003; Saint-Hilaire & Benz 2005), we see from Figure 5 that the energy carried by nonthermal electrons at the impulsive phase (the first peak) is adequate to account for the thermal energy content of the gradual phase (the second peak) (see also Sui et al. 2005).

4 DISCUSSION AND SUMMARY

A good example of solar flares with two peaks at the 12 – 25 keV light curve is presented. The time difference between the two peaks, on the order of 1 minute, varies with energy. The first peak looks more impulsive and is sustained for a relatively short time. There are no obvious time delays among the emissions at different energies. However, the second peak presents an obvious time delay at the lower energy relative to higher energy. Spectral fitting shows that the emissions at the first peak mostly have a non-thermal origin, while the emissions at the second peak have a thermal origin. Morphologically, the higher energy X-rays at the first peak come mainly from the footpoints of the flare loop, while the lower energy X-ray source initially evolves from the intense footpoints to the whole loop later and finally concentrates near the apex of the loop. The energy analysis shows that the non-thermal electrons which appeared at the first peak carry more energy than those in thermal form at the second peak.

All of these results strongly support the standard scenario of solar flares: the energetic electrons accelerated during the first peak (impulsive phase) carry quite large amounts of energy and deposit most of them at the footpoints of the flare loop, resulting in the first hard X-ray peak; the heated material then evaporates upward along the flare loop, and results in the second peak of X-rays when quite a large amount of the evaporated material reaches the apex of the loop. That is, the second peak does not come from the magnetic reconnection but rather from the evaporation which resulted from the input of non-thermal electrons released during the first peak. If the SXR peak (e.g., at 02:18:20 UT for 17 – 19 keV) corresponds to the moment when the last evaporated material from the footpoints reaches the apex of the loop, the mean speed of evaporation is about 570 km s^{-1} ($L/\Delta t$, where L, the length of the loop, is about 17 000 km, and Δt is about 30 s for 17 – 19 keV). This speed is comparable to those obtained by Antonucci et al. (1990) who found that the maximum values of the velocity distributions observed in Ca XIX and Fe XXV were 400 – 600 km s^{-1} and 700 – 970 km s^{-1}, respectively.

In fact, the two peaks at 12 – 25 keV in the light curve and their relationships are not a new story. The earlier observations had already revealed two such peaks (e.g., Kane & Anderson 1970). The later observations, made by HXRBS onboard SMM and BATSE on CGRO, had not covered the energy ranges of both SXRs and HXRs. So, the SXRs and HXRs were observed separately with different instruments (e.g., Veronig et al. 2002b). We checked the *RHESSI* flare list for 2002 and found that the number of flares showing two peaks at 12 – 25 keV is only several percent. Although the percentage is so low, we believe that this kind of flare reflects the fundamental nature of a solar flare. Physically, if the nonthermal energy inputs for a rather long time, longer than the time required for evaporated material filling the loop, or the flare involves several inputs of nonthermal energies, both the thermal and nonthermal emissions could not be distinguished as two separate peaks in the 12 – 25 keV light curves. Furthermore, if thermal energy release plays an important role (e.g., Dennis & Zarro 1993; Gan et al. 1993), the flares with two peaks in the 12 – 25 keV light curve cannot be expected. Recently, Hannah et al. (2008) studied a small flare which could be attributed to this kind of flare.

The statistical results given by Li & Gan (2006), Veronig et al. (2002b), and the results presented in this paper all demonstrated that, for some events, the maximum of soft X-ray emission happens at some time after the end of the nonthermal energy input. The time difference seems to be comparable to the moment when the last evaporated material reaches the apex of the loop, where the kinetic energy is transformed into thermal energy. A simple estimation shows that the ratio of the kinetic energy to thermal energy can be as large as 60% with an assumption of evaporated velocity 500 km s^{-1} and temperature 2×10^7 K. This time difference does not seem to be consistent with the classic Neupert effect (e.g., Neupert 1968) which requires that the nonthermal energy instantly transforms into thermal energy, and that soft X-rays reach the maximum just at the moment when the hard X-rays stop. We therefore propose a modified Neupert effect as follows:

$$F_{\mathrm{SXR}}(t) \propto \int^{t} F_{\mathrm{HXR}}(t_x - \tau)dt_x \quad \text{or} \quad \frac{d}{dt}F_{\mathrm{SXR}}(t) \propto F_{\mathrm{HXR}}(t-\tau),$$

where τ is a parameter which may be a comprehensive consequence of some complicated processes, including the filling of the loop by evaporated material. To systematically check the Neupert effect with the above improvement could be an interesting work in the future, in which one should include more samples and focus on the values of τ and its meaning. Does τ depend on time as the atmosphere responds to flare energy deposition? Does τ depend on the length of flaring loops? Does τ depend on the density of flaring loops? What is the relationship between τ and the temporal behavior of flare energy release? Before we answer all of these questions, the modified Neupert effect only remains a suggestion, although it seems to be able to explain more events, especially for the case in which SXRs peak later than the end time of HXRs. In parallel, future nonthermal hydrodynamic modeling could provide another valuable diagnostic.

In summary, among the *RHESSI* flare samples, we extracted some events which present two peaks in the 12 – 25 keV light curves, as discovered by Kane & Anderson (1970). By analyzing the light curves, spectra, and images for such a *RHESSI* flare, we showed the expected causal relationship between these two peaks. The time difference between the peak of SXRs and the end of HXRs suggests that the classic expression of the Neupert effect should be modified to include a time delay.

Acknowledgements This work is supported by the National Natural Science Foundation of China (Grant Nos. 10773031 and 10833007), the Ministry of Science and Technology of China (Grant No. 2006CB806302), and by the CAS project KJCX2-YW-T04.

References

Antonucci, E., Dodero, M. A., & Martin, R. 1990, ApJS, 73, 147
Antonucci, E., Gabriel, A. H., & Dennis, B. R. 1984, ApJ, 287, 917
Aschwanden, M. J. 2004, Physics of the Solar Corona. An Introduction (Praxis Publishing Ltd., Chichester, UK, and Springer-Verlag Berlin)
Aschwanden, M. J. 2007, ApJ, 661, 1242
Aschwanden, M. J., Brown, J. C., & Kontar, E. P. 2002, Solar Phys., 210, 383
Brosius, J. W., & Holman, G. D. 2007, ApJ, 659, L73
Brown, J. C. 1971, Solar Phys., 18, 489
Dennis, B. R., & Zarro, D. M. 1993, Solar Phys., 146, 177
Dennis, B. R., Veronig, A., Schwartz, R. A., Sui, L., Tolbert, A. K., Zarro, D. M., & Rhessi Team 2003, Adv. Space Res., 32, 2459
Emslie A. G., et al. 2004, J. Geophys. Res., 109, 10104
Fisher, G. H., Canfield, R. C., & McClymont, A. N. 1985, ApJ, 289, 425
Gan, W. Q., Fang, C., & Zhang, H. Q. 1991, A&A, 241, 618
Gan, W. Q., & Li, Y. P. 2002, Adv. Space Res., 30, 683
Gan, W. Q., Li, Y. P., & Chang, J. 2001, ApJ, 552, 858
Gan, W. Q., Rieger, E., & Fang, C. 1993, ApJ, 416, 886
Hannah, I. G., Krucker, S., Hudson, H. S., Christe, S., & Lin, R. P. 2008, A&A, 481, L45
Holman, G. D., Sui, L., Schwartz, R. A., & Emslie, A. G. 2003, ApJ, 595, L97
Hurford, G. J., et al. 2002, Solar Phys., 210, 61
Jiang, Y. W., Liu, S., Liu, W., & Petrosion, V. 2006, ApJ, 638, 1140
Jin, M., & Ding, M. D. 2007, A&A, 471, 705
Kane, S. R., & Anderson, K. A. 1970, ApJ, 162, 1003
Li, Y. P., & Gan, W. Q. 2006, ApJ, 652, L61

Lin, R. P., et al. 2002, Solar Phys., 210, 3
Lin, R. P., & Hudson, H. S. 1976, Solar Phys., 50, 153
Liu, W., Liu, S., Jiang, Y. W., & Petrosian, V. 2006, ApJ, 649, 1124
Milligan, R. O., Callagher, P. T., Mathioudakis, M., Bloomfield, D. S., Keenan, F. P., & Schwartz, R. A. 2006, ApJ, 638, L117
Neupert, W. M. 1968, ApJ, 153, L59
Saint-Hilaire, P., & Benz, A. O. 2005, A&A, 435, 743
Smith, D. M., et al. 2002, Solar Phys., 210, 33
Sui, L., Holman, G. D., & Dennis, B. R. 2005, ApJ, 626, 1102
Sui, L., Holman, G. D., & Dennis, B. R. 2006, ApJ, 645, L157
Sui, L., Holman, G. D., & Dennis, B. R. 2007, ApJ, 670, 862
Teriaca, L., Falchi, A., Cauzzi, G., Falciani, R., Smaldone, L. A., & Andretta, V. 2003, ApJ, 588, 596
Veronig, A. M., Brown, J. C., Dennis, B. R., Schwartz, R. A., Sui, L., & Tolbert, A. K. 2005, ApJ, 621, 482
Veronig, A., Temmer, M., Hanslmeier, A., Otruba, W., & Messerotti, M. 2002a, A&A, 382, 1070
Veronig, A., Vršnak, B., Dennis, B. R., Temmer, M., Hanslmeier, A., & Magdalenić, J. 2002b, A&A, 392, 699
Veronig, A., Vršnak, B., Temmer, M., & Hanslmeier, A. 2002c, Solar Phys., 208, 297